

# Shift of Dirac points and strain induced pseudo-magnetic field in graphene

Hua Tong Yang\*

Center for Advanced Optoelectronic Functional Materials Research,  
Key Laboratory for UV-Emitting Materials and Technology of Ministry of Education,  
and School of Physics, Northeast Normal University, Changchun 130024, China

We propose that the strain induced effective pseudo-magnetic field in graphene can also be explained by a curl movement of the Dirac points, if the Dirac points can be regarded as a slowly varying function of position. We also prove that the Dirac points must be confined within two triangles, each one has 1/8 the area of the Brillouin zone

PACS numbers: 73.22.Pr, 73.22.Dj, 73.22.Gk, 73.20.At

The discovery of graphene, a monolayer carbon atom sheet [1], and the development of experimental technique to manipulate this two-dimensional(2D) material have ignited intense interest in this system [2–5]. One of the most attractive characters of graphene is that its low energy excitation satisfies a massless 2D Dirac equation [6], and the chemical potential crosses its Dirac points(or Fermi points) in neutral graphene. These special characters lead to many unusual properties and new phenomena [5, 7–9], such as the anomalous integer quantum Hall effect(QHE) [8, 9]. Recently, experiments have confirmed another remarkable effect that mechanical strain can induce a very strong effective pseudo-magnetic field, leading to a pseudo-QHE, which can be observed in zero magnetic field [10, 11]. In this paper we propose that the strain induced effective vector potential can also be explained by shift  $\delta\mathbf{K}(\mathbf{x})$  of the Dirac points  $\mathbf{K}(\mathbf{x})$ , its effective pseudo-magnetic field is in proportion to  $\nabla \times \mathbf{K}(\mathbf{x})$ , only if the Dirac points  $\mathbf{K}(\mathbf{x})$  can be regarded as a slowly varying function of position, and the Fermi velocity is generalized to a tensor[12]. We also prove that the Dirac points can not be arbitrarily moved, they must be confined within two triangles, each one has 1/8 the area of the Brillouin zone(BZ).

Firstly, consider a tight-binding Hamiltonian describing a uniformly deformed honeycomb lattice with three different nearest-neighbor hopping energies  $t_1, t_2, t_3$ [13–15]:

$$\hat{H} = - \sum_{\langle \mathbf{i}, \mathbf{j} \rangle} t_{\mathbf{i}, \mathbf{j}} c_{\mathbf{i}a}^\dagger c_{\mathbf{j}b} + h.c., \quad (1)$$

where  $c_{\mathbf{j}b}$  ( $c_{\mathbf{i}a}^\dagger$ ) are annihilation(creation) operators,  $\mathbf{i}(\mathbf{j})$  are position vectors of unit cells,  $a(b)$  denote two inequivalent atoms in a unit cell,  $t_{\mathbf{i}, \mathbf{j}}$  is the electronic hopping energy from the  $\mathbf{j}$ th unit cell  $b$  atom to  $\mathbf{i}$ th unit cell  $a$  atom. Suppose that the deformed lattice remains invariant under spatial translation, i.e.,  $t_{\mathbf{i}, \mathbf{j}}$  only depends on  $\mathbf{i} - \mathbf{j}$ , but the three nearest-neighbor hopping energies  $t_{1,2,3}$  may be different owing to anisotropy of strains, as shown in Fig.1. The hopping parameters can be written as some  $2 \times 2$  matrixes  $\mathbf{t}(\mathbf{i} - \mathbf{j})$ , whose elements are defined by  $[\mathbf{t}(\mathbf{i} - \mathbf{j})]_{a,b} \equiv t_{\mathbf{i}, \mathbf{j}}$ . For this nearest-neighbor

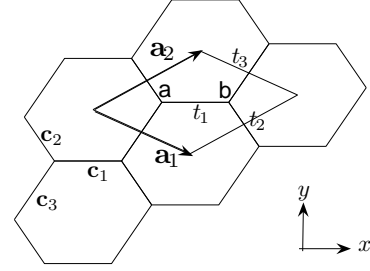


FIG. 1: Unit cell and hopping parameters for deformed graphene.

tight-binding Hamiltonian, the non-vanishing hopping matrixes are

$$\mathbf{t}(0) = \begin{pmatrix} 0 & t_1 \\ t_1 & 0 \end{pmatrix}, \mathbf{t}(\mathbf{a}_1) = \begin{pmatrix} 0 & t_2 \\ 0 & 0 \end{pmatrix}, \mathbf{t}(\mathbf{a}_2) = \begin{pmatrix} 0 & t_3 \\ 0 & 0 \end{pmatrix} \quad (2)$$

and  $\mathbf{t}(-\mathbf{a}_1) = \mathbf{t}^\dagger(\mathbf{a}_1)$ ,  $\mathbf{t}(-\mathbf{a}_2) = \mathbf{t}^\dagger(\mathbf{a}_2)$ . By Fourier transformation

$$c_{\mathbf{j}, a(b)} = \frac{1}{\sqrt{N}} \sum_{\mathbf{k}} c_{\mathbf{k}, a(b)} \exp(i\mathbf{k} \cdot \mathbf{j})$$

with  $N$  a normalization constant, the Hamiltonian (1) can be cast into the form

$$\hat{H} = - \sum_{\mathbf{k}} [c_{\mathbf{k}, a}^\dagger, c_{\mathbf{k}, b}^\dagger] \begin{bmatrix} h_{aa}(\mathbf{k}) & h_{ab}(\mathbf{k}) \\ h_{ba}(\mathbf{k}) & h_{bb}(\mathbf{k}) \end{bmatrix} \begin{bmatrix} c_{\mathbf{k}, a} \\ c_{\mathbf{k}, b} \end{bmatrix}, \quad (3)$$

where  $h_{aa}(\mathbf{k}) = h_{bb}(\mathbf{k}) = 0$ ,  $h_{ab}(\mathbf{k}) = h_{ba}^*(\mathbf{k})$ , and

$$h_{ba}(\mathbf{k}) = t_1 + t_2 \exp(i\mathbf{k} \cdot \mathbf{a}_1) + t_3 \exp(i\mathbf{k} \cdot \mathbf{a}_2), \quad (4)$$

with  $\mathbf{a}_1, \mathbf{a}_2$  the lattice unit vectors. The energy bands obtained by diagonalizing this Hamiltonian are[16]

$$E_{\pm}(\mathbf{k}) = \pm |t_1 + \tilde{t}_2(\mathbf{k}) + \tilde{t}_3(\mathbf{k})|, \quad (5)$$

where  $\tilde{t}_2(\mathbf{k}) = t_2 e^{i\mathbf{k} \cdot \mathbf{a}_1}$ ,  $\tilde{t}_3(\mathbf{k}) = t_3 e^{i\mathbf{k} \cdot \mathbf{a}_2}$ , the plus sign corresponds to the upper( $\pi$ ) and minus to the lower( $\pi^*$ ) band respectively. From Eq.(5) we notice that if  $\mathbf{K}$  is a zero point of  $h_{ba}(\mathbf{K})$ , i.e.,

$$t_1 + \tilde{t}_2(\mathbf{K}) + \tilde{t}_3(\mathbf{K}) = 0, \quad (6)$$

then  $E_+(\mathbf{k})$  and  $E_-(\mathbf{k})$  will meet at  $\mathbf{K}$ , i.e.,  $E_+(\mathbf{K}) = E_-(\mathbf{K}) = 0$ , this  $\mathbf{K}$  is known as the Dirac point. The Hamiltonian (3) can be expanded up to a linear order in  $\mathbf{p} = \mathbf{k} - \mathbf{K}$  in a neighborhood of point  $\mathbf{K}$

$$\begin{bmatrix} h_{aa}(\mathbf{k}) & h_{ab}(\mathbf{k}) \\ h_{ba}(\mathbf{k}) & h_{bb}(\mathbf{k}) \end{bmatrix} \simeq \begin{bmatrix} 0 & \vec{\alpha}^* \cdot \mathbf{p} \\ \vec{\alpha} \cdot \mathbf{p} & 0 \end{bmatrix} = v_{\mu\nu} \sigma^\mu p^\nu, \quad (7)$$

where  $\mu, \nu = 1, 2$  denote two components of a 2D vector and a sum over the repeated indices  $\mu, \nu$  is implied,  $\vec{\alpha}$  is a complex vector with  $\text{Re}(\vec{\alpha}) = (v_{11}, v_{12})$ ,  $\text{Im}(\vec{\alpha}) = (v_{21}, v_{22})$ ,  $\sigma^{1,2}$  are Pauli matrixes acting on the sublattice degree of freedom, tensor  $v_{\mu\nu}$  represents the anisotropy of the dispersion near the Dirac points, it only occurs noticeable departure from  $v_F \delta_{\mu\nu}$  in a strongly deformed graphene[12]. However, after this modification the strain induced effective vector potential will acquire a direct physical meaning. For a graphene under nonuniform but slowly varying strain,  $t_i(\mathbf{x})$  and hence the Dirac point  $\mathbf{K}(\mathbf{x})$  as well as  $v_{\mu\nu}(\mathbf{x})$  can be regarded as some smooth functions of position  $\mathbf{x}$ , the local linearized Hamiltonian  $v_{\mu\nu} \sigma^\mu (k^\nu - K^\nu(\mathbf{x}))$  on the RHS of Eq.(7) can be cast into

$$v_{\mu\nu}(\mathbf{x}) \sigma^\mu (p^\nu - \delta K^\nu(\mathbf{x})), \quad (8)$$

where  $\mathbf{p} - \delta \mathbf{K}(\mathbf{x}) \equiv \mathbf{k} - \mathbf{K}(\mathbf{x})$ ,  $\delta \mathbf{K}(\mathbf{x}) \equiv \mathbf{K}(\mathbf{x}) - \mathbf{K}_f$  with  $\mathbf{K}_f$  the corresponding Dirac point in strain-free graphene. Unlike the usual explanation of the strain induced gauge field in graphene[5, 17], where the effective vector potential is an auxiliary quantity and describes the mixed effects of both anisotropy of  $v_{\mu\nu}$  and the shift of Dirac point, here the vector potential only represents the relative translation of the Dirac points,  $(e/c)\mathbf{A}(\mathbf{x}) = \delta \mathbf{K}(\mathbf{x})$ , its pseudo-magnetic field  $\mathbf{B}(\mathbf{x}) = (c/e)\nabla \times \mathbf{K}(\mathbf{x})$ , and the physical effects are mainly determined by the pseudo-magnetic flux through a loop  $(c/e) \oint_L \mathbf{K}(\mathbf{x}) \cdot d\mathbf{x}$ . In the following sections we shall discuss the properties of  $\mathbf{K}(\mathbf{x})$ , and illustrate how a curl field  $\mathbf{K}(\mathbf{x})$  is induced by a strain.

From Eq.(6) we know that the vectors representing  $t_1, \tilde{t}_2(\mathbf{K}), \tilde{t}_3(\mathbf{K})$  in the complex plane can form a directed triangle for a Dirac point  $\mathbf{K}$ , as illustrated in Fig.2a. According to the triangle inequality, we have the following necessary and sufficient conditions for the existence of the Dirac points[13]:

$$t_1 + t_2 \geq t_3, \quad t_2 + t_3 \geq t_1, \quad t_3 + t_1 \geq t_2. \quad (9)$$

These conditions define a pyramidal domain in the  $(t_1, t_2, t_3)$  space, shown in Fig.2b. If  $t_1, t_2, t_3$  satisfy inequalities (9), then there exists two directed triangles with the same edges  $t_1, t_2, t_3$  but different possible orientations, which determine two angles  $\theta_1, \theta_2$  satisfying  $t_1 + t_2 e^{i\theta_1} + t_3 e^{i\theta_2} = 0$ , where  $\theta_1, \theta_2$  are given by the law of cosine

$$\begin{aligned} \theta_{\pm 1} &= \pm \left[ \pi - \arccos \left( \frac{t_1^2 + t_2^2 - t_3^2}{2t_1 t_2} \right) \right], \\ \theta_{\pm 2} &= \pm \left[ \arccos \left( \frac{t_1^2 + t_3^2 - t_2^2}{2t_1 t_3} \right) - \pi \right]. \end{aligned} \quad (10)$$

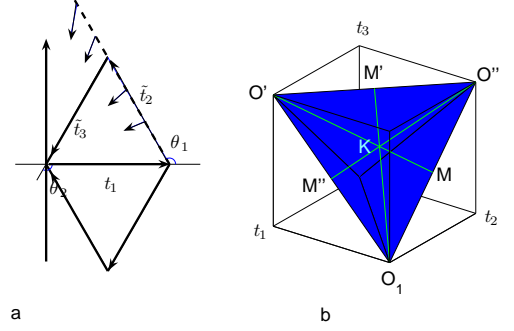


FIG. 2: (color online). (a) Zero points of  $h_{ba}(\mathbf{k})$  determine two directed triangles with edges  $t_{1,2,3}$  in the complex plane. For a given  $t_1$  and a fixed direction of  $\tilde{t}_2$ , the arguments of  $\tilde{t}_3$  must satisfy conditions (15) to ensure  $t_{2,3} \geq 0$ . (b) Dirac points exist if  $t_i$  satisfy inequalities (9), which describe a pyramidal domain in  $(t_1, t_2, t_3)$  space, if  $(t_1, t_2, t_3)$  goes beyond this domain, an energy gap will be opened.

Thus the Dirac points  $\mathbf{K}$  can be determined by letting

$$\exp(i\mathbf{K} \cdot \mathbf{a}_1) = \exp(i\theta_1), \quad \exp(i\mathbf{K} \cdot \mathbf{a}_2) = \exp(i\theta_2), \quad (11)$$

so we have

$$\mathbf{K} = \frac{1}{2\pi} (\theta_1 \mathbf{b}_1 + \theta_2 \mathbf{b}_2) + \mathbf{K}_0, \quad (12)$$

with  $\mathbf{b}_1, \mathbf{b}_2$  the reciprocal lattice vectors defined by  $\mathbf{a}_i \cdot \mathbf{b}_j = 2\pi \delta_{ij}$ , and  $\mathbf{K}_0 = n\mathbf{b}_1 + m\mathbf{b}_2$  with  $n, m$  are arbitrary integers. Notice that if  $t_1 + \tilde{t}_2 + \tilde{t}_3 = 0$ , then  $t_1 + \tilde{t}_2^* + \tilde{t}_3^* = 0$ , this implies that there exists two Dirac points  $\mathbf{K}(\mathbf{x})$  and  $-\mathbf{K}(\mathbf{x})$ . However, if  $(t_1, t_2, t_3)$  exactly locates on the boundary surface of the pyramid, e.g.,  $t_1 = t_2 + t_3$ , then the two triangles will mutually coincide and  $\tilde{t}_2 = \tilde{t}_2^*, \tilde{t}_3 = \tilde{t}_3^*$  (see Fig.2a), hence  $\mathbf{K}(\mathbf{x})$  and  $-\mathbf{K}(\mathbf{x})$  become equivalent, and  $\vec{\alpha} = i(t_2 \mathbf{a}_1 + t_3 \mathbf{a}_2)$  becomes a pure imaginary vector, so the Fermi velocity in the directions perpendicular to  $\vec{\alpha}$  vanishes (Fig.3b and 3d)[14, 15, 18]. If  $(t_1, t_2, t_3)$  goes beyond the domain defined by Eq.(9), e.g.,  $t_1 > t_2 + t_3$ , Eq.(6) will have no any root, an energy gap with magnitude  $E_g = 2(t_1 - t_2 - t_3)$  will occur at the corresponding points  $\mathbf{K}_{\pm} = \pm 1/2(\mathbf{b}_1 + \mathbf{b}_2)$  (see Fig.3c)[19], and the effective Hamiltonian (8) must be further modified by adding a mass term and some second order terms.

Another important property is the range of  $\mathbf{K}(\mathbf{x})$ . We shall prove that the Dirac points must be confined within some special regions of the BZ. To this end, notice that if a Dirac point  $\mathbf{K} = (1/2\pi)(\theta_1, \theta_2)$  is given, then its associated  $t_{1,2,3}$  can also be determined up to an arbitrary factor, except six special cases of  $\theta_1, \theta_2 = 0, \pm\pi$  (see Fig. 2a). If  $\theta_1, \theta_2 \neq 0, \pm\pi$ . According to the law of sines we have

$$\frac{t_2}{t_1} = \frac{\sin \theta_2}{\sin(\theta_1 - \theta_2)}, \quad \frac{t_3}{t_1} = \frac{\sin \theta_1}{\sin(\theta_2 - \theta_1)}, \quad (13)$$

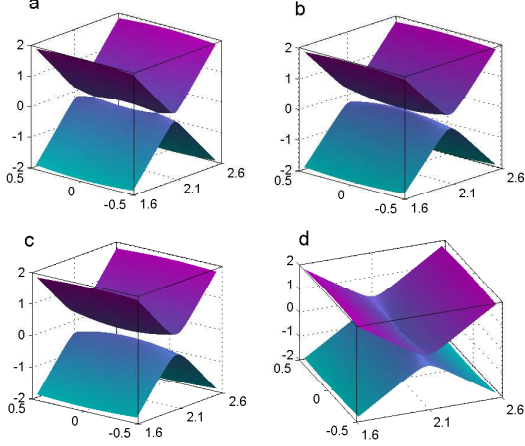


FIG. 3: (color online) (a) Energy band when two Dirac points are very close, where  $t_1 = 2.8, t_{2,3} = 1.45$ , (b), (d)  $t_1 = 2.8, t_{2,3} = 1.4$ , two Dirac points are equivalent(superposed), (c)  $t_1 = 2.8, t_{2,3} = 1.35$ , an energy gap occurs.

or

$$(t_1, t_2, t_3) \propto (\sin(\theta_2 - \theta_1), -\sin \theta_2, \sin \theta_1). \quad (14)$$

For the six special cases we have: if  $(\theta_1, \theta_2) = \pm(\pi, \pi)$ ,  $t_1 = t_2 + t_3$ ; if  $(\theta_1, \theta_2) = \pm(\pi, 0)$ ,  $t_2 = t_1 + t_3$ ; if  $(\theta_1, \theta_2) = \pm(0, \pi)$ ,  $t_3 = t_1 + t_2$ . From Eq.(14) we can find that the  $\theta_1, \theta_2$  must satisfy some constrain conditions to guarantee  $t_{1,2,3} \geq 0$ , as illustrated in Fig.2a. For an arbitrary  $t_2$  and a fixed  $\theta_1$ (direction of  $\tilde{t}_2$ ),  $\tilde{t}_3$  must point in a direction between the directions of  $-\tilde{t}_2$  and negative real axis, i.e., argument  $\theta_1, \theta_2$  must satisfy

$$\begin{aligned} \theta_1 + \pi < \theta_2 < \pi, \quad \theta_1 \in (-\pi, 0), \\ -\pi < \theta_2 < \theta_1 - \pi, \quad \theta_1 \in (0, \pi). \end{aligned} \quad (15)$$

These two inequalities respectively determine the range of  $\mathbf{K}(\mathbf{x})$  and  $-\mathbf{K}(\mathbf{x})$ . They describe two open triangles  $\triangle MM'_1M''_1$  and  $\triangle M'M''_1M''_3$  in reciprocal space, as shown in Fig.4, each one has 1/8 the area of a unit cell of the reciprocal space(the parallelogram  $M''M''_1M''_2M''_3$ ), and each Dirac point is confined within a triangle, so, the Dirac points  $\mathbf{K}$  and  $-\mathbf{K}$  can meet(become equivalent) only at the vertexes of  $\triangle MM'_1M''_1$  and  $\triangle M'M''_1M''_3$ . The remaining hexagon(blue in Fig.4) is a forbidden region for the Dirac points. This confinement also limits the order of magnitude of  $\nabla \times \mathbf{K}(\mathbf{x})$ , i.e., the strain induced pseudo-magnetic field. In order to show the underlying regularity, here we have ignored the variations of  $\mathbf{b}_1, \mathbf{b}_2$  with the deformation of lattice, and simply sketch all  $\mathbf{K} = (k_1, k_2)$  in the same affine frame. After translating to the first BZ of graphene,  $\triangle MM'_1M''_1$  and  $\triangle M'M''_1M''_3$  are equivalent to a ringlike region consists of six triangles  $\triangle MKM'_1$ ,  $\triangle M_1K_2M''_2$ ,  $\triangle M''K_1M'$ , etc.

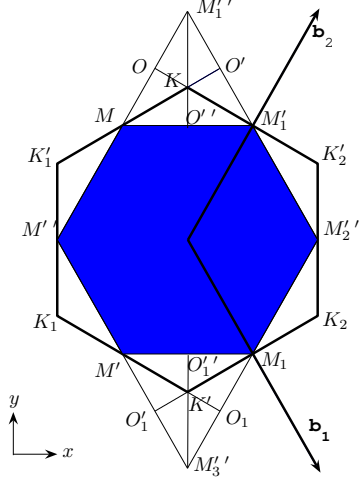


FIG. 4: (color inline) Rang of the Dirac points consists of six triangles in first the BZ, or  $\triangle MM'_1M''_1$  and  $\triangle M'M''_1M''_3$ .

In order to illustrate how a non-vanishing  $\nabla \times \mathbf{K}$  is induced by strain, we only need to analyze three ideal cases, in which only one  $t_i$  is slightly changed,  $t_i \rightarrow t_0 + \delta t_i$ , while the other two  $t_{j,k}$  remain constant,  $t_j = t_k = t_0$ , which can also be roughly regarded as that the bond  $\mathbf{c}_i$  is elongated(or compressed) while the other two bonds  $\mathbf{c}_j, \mathbf{c}_k$  and their directions remain fixed(see Fig.5b). Notice that the Dirac points only depend on the relative proportions of  $t_1, t_2, t_3$ , so, as an equivalent case, we can always assume that  $t_1$  remains constant and only  $t_2, t_3$  are variables. Moreover, in these equivalent cases the  $\tilde{t}_2$  and  $\tilde{t}_3$  can be determined by the end of the vector  $t_1 + \tilde{t}_2 = -\tilde{t}_3$ , denoted by  $P$  in Fig.5a. So, we can represent the variation of the Dirac points by the shift of the point  $P$ . To this end, we have to determine the corresponding  $P$  of the three classes of characteristic points in the range of the Dirac points: (1)  $K$ (or  $K'$ ) etc.(see Fig.4), according to Eq.(13), Dirac points locate at these two points only if  $t_1 = t_2 = t_3$ , their corresponding  $P$  is located at  $K$ (or  $K'$ ) in Fig.5a; (2) critical points  $M(M_1) = (\pm 1/2, 0)$ ,  $M'(M'_1) = (0, \pm 1/2)$ , and  $M''(M''_1) = (\pm 1/2, \pm 1/2)$ , in these cases there exist only one Dirac point since the points  $\mathbf{K}$  and  $-\mathbf{K}$  are equivalent, their corresponding  $(t_1, t_2, t_3)$  are located on the boundary of the pyramidal domain, while their corresponding  $P$  are located at the real axis in Fig.5a; (3)  $O, O', O''$  etc., their corresponding  $P$  are the centers of two circles and the infinite limit points of the straight line  $KK'$  in Fig.5a, which respectively correspond to the limits of  $t_2 \rightarrow 0, t_3 \rightarrow 0$  and  $t_1 \rightarrow 0$ (equivalent to  $t_2 = t_3 \rightarrow \infty$ ). Now we analyze the shifts of the Dirac points in the three ideal situations. (1)  $t_1, t_2$  remain constant and  $t_2 = t_1$ , only  $t_3$  is variable, the trajectory of the corresponding  $P$  is a circle with radius  $t_1$  and centered

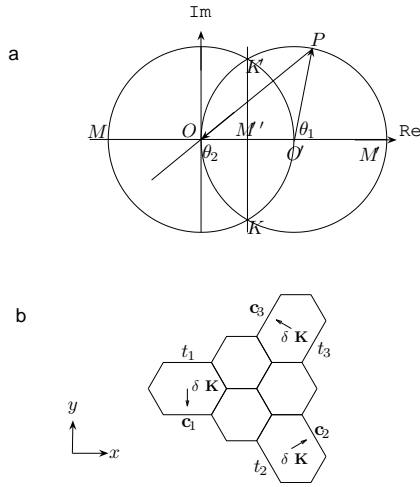


FIG. 5: (a) The trajectories of P in three ideal cases. (b) A schematic diagram of the shift of Dirac point  $\delta\mathbf{K}$  and its curl,  $\delta\mathbf{K}$  perpendicular to  $\mathbf{c}_i$ , if bond  $\mathbf{c}_i$  is slightly elongated.

at the point  $(t_1, 0)$  in Fig.5a, so the arguments  $(\theta_1, \theta_2)$  satisfy

$$\begin{aligned} \theta_1 - 2\theta_2 - 2\pi &= 0, & \theta_1 &\in (-\pi, 0), \\ \theta_1 - 2\theta_2 + 2\pi &= 0, & \theta_1 &\in (0, \pi). \end{aligned} \quad (16)$$

They describe line segments  $M'O_1$  and  $M'_1O$  in Fig.4; (2)  $t_3(=t_1)$  remain constant while  $t_2$  is variable, the trajectory of corresponding P is another circle with radius  $t_1$  centered at the origin, its associated  $(\theta_1, \theta_2)$  satisfy

$$\begin{aligned} \theta_2 - 2\theta_1 + 2\pi &= 0, & \theta_2 &\in (-\pi, 0), \\ \theta_2 - 2\theta_1 - 2\pi &= 0, & \theta_2 &\in (0, \pi), \end{aligned} \quad (17)$$

which describe  $MO'$  and  $M_1O'_1$  in Fig.4; (3)  $t_1$  remains constant while  $t_2, t_3$  are variable but  $t_2 = t_3$  (or vice versa,  $t_1$  is variable,  $t_2(=t_3)$  remain constant), the trajectory of P is straight line  $KK'$ ,  $(\theta_1, \theta_2)$  satisfy

$$\theta_1 + \theta_2 = 0, \quad \frac{\pi}{2} < |\theta_1| < \pi, \quad (18)$$

which describe  $M''_1O''$  and  $M''_3O''_1$  in Fig.4. Summarizing Eqs.(16)(17)(18) and comparing with Fig.4, we observe that if a band, e.g.,  $\mathbf{c}_1$  is slightly elongated (or compressed) along its direction,  $\mathbf{c}_1 \rightarrow (1 + \delta)\mathbf{c}_1$ , while the other two bonds  $\mathbf{c}_2, \mathbf{c}_3$  remain fixed, then  $t_1$  will be slightly changed while  $t_2(=t_3)$  remain constant, the Dirac point  $\mathbf{K}$  will be slightly moved in the direction perpendicular to  $\mathbf{c}_1$ , i.e.,  $\delta K_y \neq 0$  (see Fig.4,  $K$  moves towards  $O''$  if  $t_1$  decreases, towards  $M''_1$  if  $t_1$  increases),  $\mathbf{K}'(= -\mathbf{K})$  is moved in the opposite direction. Thus, if the elongation of  $\mathbf{c}_1$  is slowly varying in the x-direction, i.e.,  $\partial t_1 / \partial x \neq 0$ , then  $\partial K_y / \partial x \neq 0$ , the other two cases are similar. So, a nonuniform strain as schematically shown in Fig.5b can induce a curl field  $\mathbf{K}(\mathbf{x})$ ,  $\nabla \times \mathbf{K} \neq 0$ .

We thank Yugui Yao, Chengshi Liu, Yichun Liu for their helpful discussions. This work was supported by the National Science Foundation of China (Grant Nos.10974027, 50725205, 50832001).

\* Electronic address: yanght653@nenu.edu.cn

- [1] K. S. Novoselov, A. K. Geim, S. V. Morozov, D. Jiang, Y. Zhang, S. V. Dubonos, I. V. Gregorieva, and A. A. Firsov, *Science* **306**, 666(2004); K. S. Novoselov, D. Jiang, F. Schedin, T. J. Booth, V. V. Khotkevich, S. M. Morozov, A. K. Geim, *Proc. Natl. Acad. Sci.* **102**, 10451(2005).
- [2] M. A. H. Vozmediano, M. P. Lopez-Sancho, and F. Guinea, *Phys. Rev. Lett.* **89**, 166401(2002).
- [3] J.C. Meyer, K. Geim, M.I. Katsnelson, K.S. Novoselov, T.J. Booth, and S. Roth, *Nature* **446**, 60(2007).
- [4] A.K. Geim, and K.S. Novoselov, *Nature Materials* **6**, 183(2007); C.W.J. Beenakker, *Rev. Mod. Phys.* **80**, 1337(2008).
- [5] A. H. Castro Neto, F. Guinea, N. M. R. Peres, K. S. Novoselov, and A. K. Geim, *Rev. Mod. Phys.* **81**, 109(2009).
- [6] G. W. Semenoff, *Phys. Rev. Lett.* **53**, 2449(1984).
- [7] V. P. Gusynin, and S. G. Sharapov, *Phys. Rev. Lett.* **95**, 146801(2005); V. P. Gusynin, V. A. Miransky, and S. G. Sharapov, *Phys. Rev. B* **74**, 195429(2006).
- [8] K. S. Novoselov, A. K. Geim, S. V. Morozov, D. Jiang, M. I. Katsnelson, I. V. Gregorieva, S. V. Dubonos, and A. A. Firsov, *Nature* **438**, 197(2005).
- [9] Y. Zhang, Y.-W. Tan, H. L. Stormer, and P. Kim, *Nature* **438**, 201(2005).
- [10] F. Guinea, M. I. Katsnelson, and A. K. Geim, *Natur Physics* **6**, 30(2010).
- [11] N. Levy, S.A.Burke, K.L.Meaker, M.Panllassigui, A.Zettl, F.Guinea, and A.H. Crommie, *Science* **329**, 544 (2010).
- [12] S. L. Zhu, B. Wang, and L.-M. Duan, *Phys. Rev. Lett.* **98**, 260402(2007); O. Bahat-Treidel, O. Peleg, M. Grobman, N. Shapira, M. Segev, and T. Pereg-Barnea, *Phys. Rev. Lett.* **104**, 063901(2010).
- [13] Y. Hasegawa, R. Konno, H. Nakano, and M. Kohmoto, *Phys. Rev B* **74**, 033413(2006).
- [14] P. Dietl, F. Piéchon, and G. Montambaux, *Phys. Rev. Lett.* **100**, 236405(2008).
- [15] G. Montambaux, F. Pichon, J.-N. Fuchs, and M. O. Goerbig, *Phys. Rec. B* **80**, 153412(2009); G. Montambaux, F. Pichon, J.-N. Fuchs and M. O. Goerbig, *Eur. Phys. J. B* **72**, 509(2009).
- [16] P. R. Wallace, *Phys. Rev.* **71**, 622(1947).
- [17] C.L.Kane and E.J.Mele *Phys. Rev. Lett.* **78**, 1932(1997); H. Suzuura and T. Ando, *Phys. Rev. B* **65**, 235412(2002); J.L.Mañe, *Phys. Rev. B* **76**, 045430(2007).
- [18] V.M. Pereira, A.H. Castro Neto, and N.M.R. Peres, *Phys. Rev. B* **80**, 045401(2009).
- [19] Other mechanisms of gap opening see e.g., S.Y. Zhou, G.H.Gweon, A.V. Fedorov, P.N.First, W.A.De Heer, D.H.Lee, F.Guinea, A.H.Castro Neto, and A.Lanzara, *Nature Materials* **6**, 770(2007); G. Giovannetti, P. A. Khomyakov, G. Brocks, P.J. Kelly, and J. van den Brink, *Phys. Rev. B* **76**, 073103(2007); R. Martinazzo, S. Casolo, and G. F. Tantardini, *Phys. Rev. B* **81**, 245420(2010).